# 锂离子电池正极材料层状 $LiNi_{1/2}Mn_{1/2}O_2$ 的制备与表征

王殿龙*,[1] 李建忠[1,2] 戴长松[1] 宋振伦[2]
([1]哈尔滨工业大学应用化学系,哈尔滨 150001)
([2]中国科学院宁波材料技术与工程研究所,宁波 315201)

**摘要**: 用一种简单的共沉淀法制备出了层状 $LiNi_{1/2}Mn_{1/2}O_2$ 材料,并且用 XRD、SEM、循环充放电、循环伏安(CV)和电化学阻抗谱(EIS)等方法对材料进行了表征测试。首先,用共沉淀法制备氢氧化镍和氢氧化锰的混合物;然后,对共沉淀溶液进行预氧化来制备前驱体;最后,用预氧化的前驱体合成了 $LiNi_{1/2}Mn_{1/2}O_2$ 材料。SEM 和 XRD 测试结果分别表明:$LiNi_{1/2}Mn_{1/2}O_2$ 材料是粒径范围在 100~200 nm 之间的球形粒子,并且具有非常好的层状结构。循环充放电表明:在空气中 900 ℃下合成时间为 9 h 的材料,在充放电截止电压为 2.8~4.6 V 的情况下,经过 40 次循环,材料的容量可以稳定地保持在 140 $mAh\cdot g^{-1}$ 左右。循环伏安曲线表明:在锂的初始脱嵌和入嵌过程中存在不可逆相变。电化学阻抗谱测试表明 $LiNi_{1/2}Mn_{1/2}O_2$ 具有很好的锂离子扩散能力。

**关键词**: 锂离子电池; 正极材料; $LiNi_{1/2}Mn_{1/2}O_2$; 共沉淀
**中图分类号**: O614.111; TM912.9 **文献标识码**: A **文章编号**: 1001-4861(2007)12-2085-06

# Synthesis and Characterization of Layered $LiNi_{1/2}Mn_{1/2}O_2$ as Cathode Material for Lithium Ion Batteries

WANG Dian-Long*,[1] LI Jian-Zhong[1,2] DAI Chang-Song[1] SONG Zhen-Lun[2]
([1]*Department of Applied Chemistry, Harbin Institute of Technology, Harbin* 150001)
([2]*Ningbo Institute of Material Technology and Engineering, Chinese Academy of Sciences, Ningbo, Zhejiang* 315201)

**Abstract:** Layered $LiNi_{1/2}Mn_{1/2}O_2$ was synthesized using a simplified co-precipitation method and characterized by XRD, SEM, charge discharge cycling, cyclic voltammetry (CV) and Electrochemistry impedance spectroscopy (EIS). Firstly, the mixture solution of the nickel hydroxide and manganese hydroxide was prepared by coprecipitation. Secondly, the precursor was prepared from the co-precipitated solution using a preoxidation method. Finally, the $LiNi_{1/2}Mn_{1/2}O_2$ was synthesized from the as-prepared precursor. The SEM and XRD results indicate that the material is composed of spherical particles with size of 100~200 nm and has well-defined layered structure. The charge discharge cycling tests reveal that the material synthesized at 900 ℃ for 9 h in air atmosphere exhibits stable capacities of about 140 $mAh\cdot g^{-1}$ in the cutoff voltage of 2.8~4.6 V for charge and discharge at the end of $40^{th}$ cycle. The CV curves show that the material has irreversible phase change at the initial state of lithium deintercalation and reintercalation processes. EIS tests show that the $LiNi_{1/2}Mn_{1/2}O_2$ has good ability of Li-ion diffusion.

**Key words:** lithium ion batteries; cathode material; $LiNi_{1/2}Mn_{1/2}O_2$; co-precipitation

收稿日期:2007-08-25。收修改稿日期:2007-10-03。
*通讯联系人。E-mail:dlwang@hit.edu.cn
第一作者:王殿龙,男,42 岁,教授,博导;研究方向:电极材料。

Since the first commercialization of lithium ion batteries in 1991, the properties of batteries have been greatly improved, but the practical cathode material mainly remains the same as the initial material $LiCoO_2$ in commercial lithium ion batteries. Because of the high cost and toxicity of Co, researchers have been devoted to develop cobalt alternatives. In recent years, lithium nickel manganese oxides have been of great interest among material chemists for advanced lithium ion batteries[1~13]. Among these materials, $LiNi_{1/2}Mn_{1/2}O_2$ is the most attractive material in terms of its low cost, high discharge capacity, long cycling stability and thermal safety[7~11]. Some efforts have been devoted to improve the electrochemical properties of $LiNi_{1/2}Mn_{1/2}O_2$ using carbon coating[14] and doping[7,15,16].

All the research results indicate that $LiNi_{1/2}Mn_{1/2}O_2$ material may have great future in the application for lithium ion batteries. But $LiNi_{1/2}Mn_{1/2}O_2$ is difficult to be synthesized by a wet method. Manganese ions in alkaline solution are easily oxidized when wet, then, manganese may exist in different oxidation states, such as $Mn^{2+}$, $Mn^{3+}$, $Mn^{4+}$, which may lead to a structural impurity in $LiNi_{1/2}Mn_{1/2}O_2$. Generally, manganese and nickel can not be dispersed uniformly in $LiNi_{1/2}Mn_{1/2}O_2$ material, thus deteriorating the properties of $LiNi_{1/2}Mn_{1/2}O_2$ as a cathode material. In this paper, we report an improved co-precipitation method for the synthesis of the $LiNi_{1/2}$ $Mn_{1/2}O_2$. A suitable precursor was obtained by an improved method with ultrasonic dispersion and preoxidation. The material with perfect performance was synthesized in terms of rechargeable capacity, rate capability, and cycle ability.

## 1 Experimental

The compound, $LiNi_{1/2}Mn_{1/2}O_2$ was synthesized by a simple mixed hydroxide method. Stoichiometric amount of nickel nitrate (A.R., Chemical Reagent Factory of Tianjin University, China) and manganese acetate (A. R., Chemical Reagent Factory of Double Boat, China) were dissolved in distilled water ($1.0\times10^{-4}$ S·m$^{-1}$). The above mixture solution was added slowly into the NaOH (A.R., Chemical Reagent Factory of Tianjin University, China) alkaline solution with vigorous stirring, at the same time the pH value of the solution was kept at 11 by dropping NaOH solution. After dropping the nickel nitrate and manganese acetate solution, $H_2O_2$ was added to the mixture solution with vigorous stirring and ultrasonic dispersing. The stirring and ultrasonic dispersing to the solution for several hours so as to oxidize the $Mn^{2+}$ to $Mn^{4+}$ as more as possible. The resulting co-precipitated nickel hydroxide and manganese dioxide were filtered out and washed thoroughly. Then, the mixture was dehydrated at 400 ℃ for 8 h to oxidize the manganese again, thus obtaining more pure $Mn^{4+}$. Then, the mixture was ground in an agate mortar with stoichiometric $LiOH\cdot H_2O$ and the powder was pressed into pellets. The pellets were calcined in air at different temperatures for several hours, followed by quenching to room temperature in air. The product was thoroughly ground for characterization and tests.

A Rigaku D/MAX-rC X-ray diffractometer with Cu $K\alpha_1$ (45 kV, 50 mA, step size=0.02°, $10°<2\theta<90°$, $\lambda$=0.154 08 nm) monochromated radiation was used to identify the crystal structure of the materials calcined under different conditions. The morphology of the samples was measured with a HITACHI S-4700 Scanning Electron Microscopy. The cyclic voltammetry test was carried out using a CHI660 electrochemical workstation (Shanghai Chenhua Ltd., China). The voltage scanning rate and scanning range was 1 mV·s$^{-1}$ and 2.6~4.6 V, respectively. The charge-discharge tests were carried out using a BTS-5 V/3 mA lithium-ion battery tester (Newear Technology Ltd., China), the current density was 60 mAh·g$^{-1}$ and the voltage range from 2.8 to 4.4, 4.5, 4.6 V. Electrochemistry impedance spectroscopy (EIS) was tested on a M273 electrochemical workstation (Princeton Applied Research Ltd., USA). The EIS was used to test the impedance of battery at different sate of charge (SOC).

The test cells were assembled as follows. The cathode was fabricated with an accurately weighed active material and conductive binder. The cathode mixtures consisted of metal oxide powder (as-prepared, 85wt% ), acetylene black (SP,10wt% ) and poly (vinylidene fluoride) (PVDF, 5wt%) was dissolved in *N*-methylpyrrolidone (NMP) solvent with stirring for 12 h,

then coated on aluminum foil. The coated cathode mixtures was dried at 120 ℃ for 12 h in an oven then cut into 1 cm diameter disks with a punch. The disk cathode was pressed with 15 MPa pressure for 2 min. Then the disk cathode was used to assemble cells. This cell was composed of a cathode and a lithium metal anode separated by a porous polypropylene film used as the separator (Celgard 3401). The electrolyte used was a 1 mol·$L^{-1}$ $LiPF_6$-ethylene carbonate (EC)/dimethyl carbonate (DMC) solution (1∶1 by volume). The cells were assembled in an argon-filled glove box.

## 2 Results and discussion

### 2.1 Characterization of materials

Fig.1 shows the XRD patterns of the $LiNi_{1/2}Mn_{1/2}O_2$ synthesized by the mixed hydroxide method at calcination temperature of 800 and 900 ℃ for 9 h, respectively. The XRD patterns can be indexed on the basis of the $\alpha$-$NaFeO_2$ type structure, space group $R\bar{3}m$ [17]. The hexagonal lattice parameters obtained by the least square fitting method.

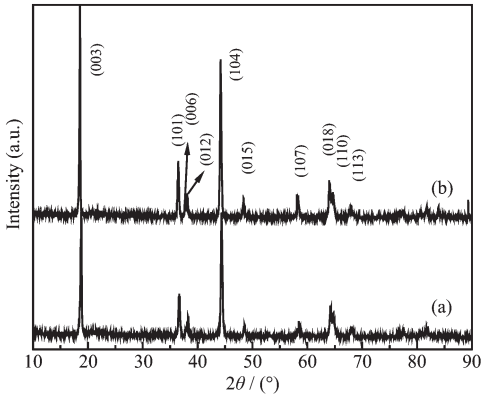


Fig.1　XRD patterns of the compound, $LiNi_{1/2}Mn_{1/2}O_2$ calcined at (a) 800 ℃; (b) 900℃

For the sample calcined at 800 ℃, the lattice parameters $a$, $c$ and $c/a$ is 0.287 2 nm, 1.425 4 nm, and 4.963, respectively, while 0.287 8 nm, 1.429 0 nm, and 4.965 for the sample calcined at 900 ℃. These parameters are in well agreement with the values reported in other references[18].

The strongest peaks of the sample calcined at 800 ℃ and 900 ℃ are (104) and (003), respectively, and the ratio $I_{(003)}/I_{(104)}$ is 0.94 and 1.16, respectively. The smaller ratio of $I_{(003)}/I_{(104)}$ possibly indicates the displacement between the transition metal ions at the 3(a) sites and lithium ions at the 3(b) sites. The nicer split (006 102) and (108 110) peak pairs in the XRD patterns (Fig.1,b) and the $c/a$ ratio > 4.93 reveal that the material calcined at 900 ℃ for 9 h has well-defined layered structure[11].

The influence of heating time and cooling patterns on the crystal structure of the samples calcined at 900 ℃ is shown in Fig.2. The XRD patterns of the samples calcined for 9 and 24 h and cooled by quenching and furnace nature cooling present sharp peaks, and indicate the high crystallinity of the samples. The calculated lattice parameters of these samples are summarized in Table 1.

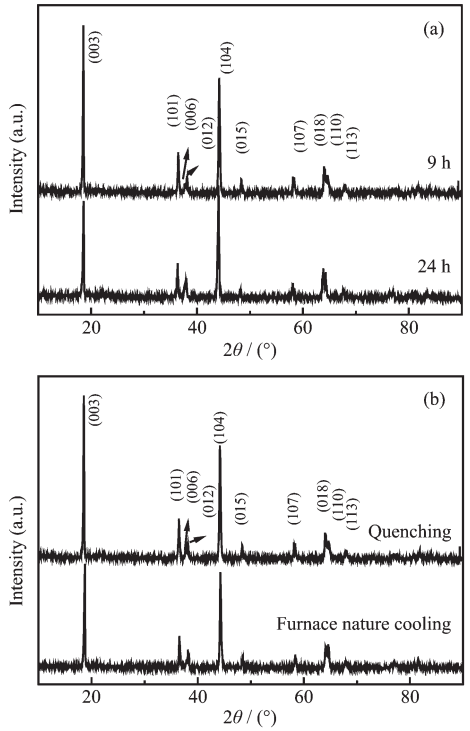


Fig.2　XRD patterns of $LiNi_{1/2}Mn_{1/2}O_2$ (a) calcined for 9 and 24 h; (b) cooled byquenching and furnace nature cooling

By comparing the calculated lattice parameters, we can know that the long time heating and the furnace-cooling can make changes in the crystal structure. We can see from the Table 1 that, under the conditions of long time heating and furnace-cooling pattern, $a$ value becomes larger and $c$ becomes smaller, the $c/a$<4.93. From the calculated results, the layered structure becomes less perfect.

**Table 1 Lattice parameters and structural parameters for $LiNi_{1/2}Mn_{1/2}O_2$**

| | Heating time / h | | Heating patterns | |
|---|---|---|---|---|
| | 9 | 24 | Quenching | Furnace-cooling |
| *a* / nm | 2.878 | 2.893 | 0.287 8 | 0.288 4 |
| *c* / nm | 1.42 90 | 1.423 8 | 1.429 0 | 1.419 7 |
| *c*/*a* | 4.965 | 4.922 | 4.965 | 4.923 |

The SEM image in Fig.3 presents the morphology of $LiNi_{1/2}Mn_{1/2}O_2$ sample synthesized at 900 ℃ for 9 h in oxygen atmosphere. The diameters of the spherical $LiNi_{1/2}Mn_{1/2}O_2$ particles are in the size range of 100~200 nm.

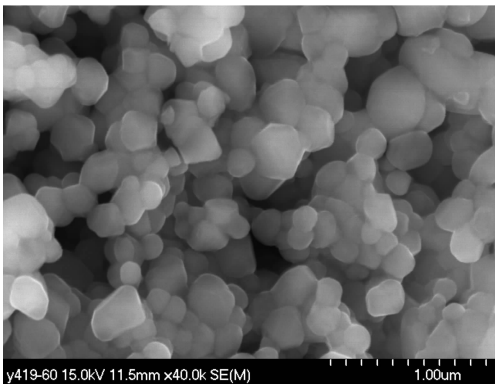


Fig.3 SEM photograph of $LiNi_{1/2}Mn_{1/2}O_2$ calcined at 900 ℃ for 9 h

## 2.2 Charge-discharge properties

Fig.4 shows the cycle performance for $LiNi_{1/2}Mn_{1/2}O_2$ synthesized under different conditions. Each curve was tested at current density of 60 mA·g$^{-1}$ and in the voltage range of 2.8~4.4 V. As can be seen from the figure, there is a very good cycle performance for the material calcined at 900 ℃ for 9 h.

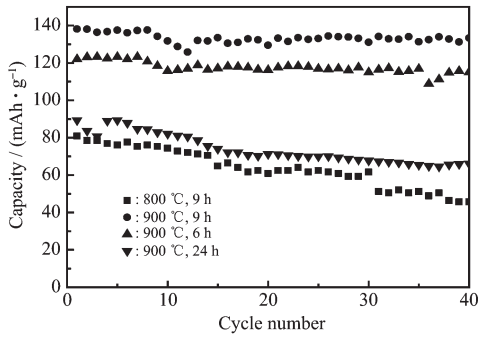


Fig.4 Cycle performance for $LiNi_{1/2}Mn_{1/2}O_2$ synthesized under different conditions

The typical charge-discharge curves for $LiNi_{1/2}Mn_{1/2}O_2$ calcined at 900 ℃ for 9 h is shown in Fig.5. The charge and discharge current is 60 mA·g$^{-1}$, as can be seen from the figure, the material has a very good reversibility. Its charge capacity (C.C.) for first cycle is 192.4 mAh·g$^{-1}$. The first cycle discharge capacity (D. C.) is found to be 133.8 mAh·g$^{-1}$. So the efficiency of the first cycle is low, about 69.5%, but the following cycling efficiency remains about 98%. The low efficiency of first cycle may be caused from the formation of solid electrolyte interphase (SEI) which consumes some active lithium.

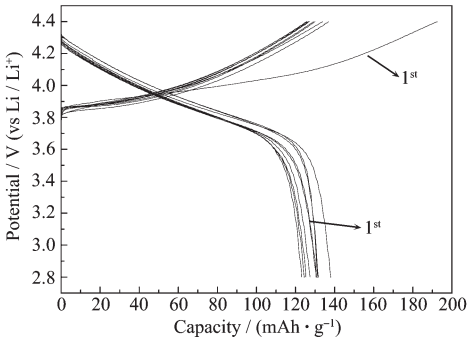


Fig.5 Typical charge and discharge curves for $LiNi_{1/2}Mn_{1/2}O_2$ synthesized at 900 ℃ for 9 h with a current of 60 mA·g$^{-1}$ at 2.8~4.4 V

Fig.6 shows the capacity-voltage relation at different cutoff voltages for charging. As can be seen, with the cutoff voltage increasing, the charge and discharge capacity increases.

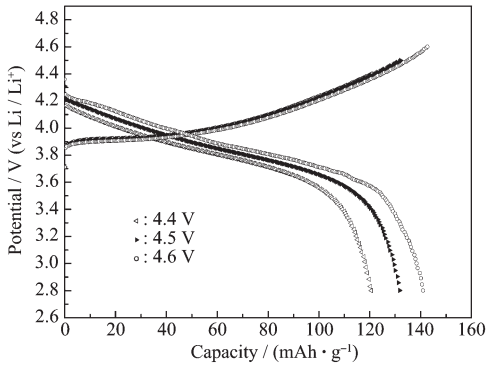


Fig.6 Charge and discharge curves in the voltage range 2.8~4.4 V, 2.8~4.5 V, 2.8~4.6 V

The material′s cycle performance in the voltage

range of 2.8~4.6 V is show in Fig.7. We can see from Fig.7 that the cutoff voltage of 4.6V for charging will not damage the electrochemical properties. At the end of 40th cycle, the capacity is almost no reduction. So the $LiNi_{1/2}Mn_{1/2}O_2$ material can be used for applications with high voltage demand.

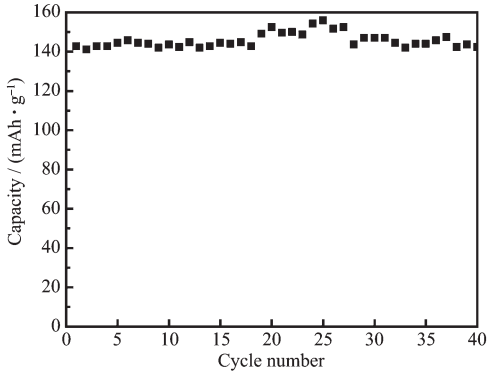


Fig.7　Cycle performance for $LiNi_{1/2}Mn_{1/2}O_2$ in the voltage range of 2.8~4.6 V with 60 mAh·g$^{-1}$ current density

## 2.3　Electrochemical properties

The CV curves for fresh cell is depicted in Fig.8.

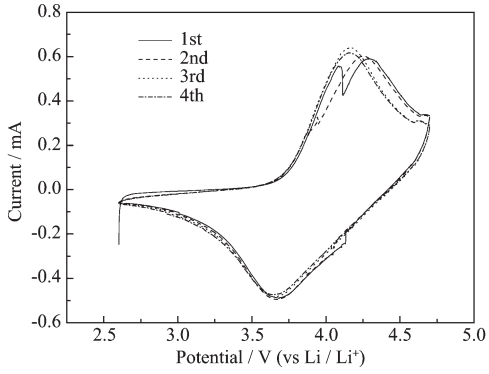


Fig.8　Cyclic voltammetry of the synthesized $LiNi_{1/2}Mn_{1/2}O_2$ in the voltage range 2.6~4.6 V at 1 mV·s$^{-1}$

It can be seen clearly that the first cycling curve have two oxidation peaks, but only one peak in the reduction process. After two cycles, two oxidation peaks become one. This may be attributed to the irreversible phase change at the start because of the existing of $Ni^{3+}$ and $Mn^{3+}$. It can be seen clearly from the figures that the major oxidation and reduction peaks are observed at around 4.15 V and 3.65 V, respectively and is representative of lithium deintercalation and reintercalation process, respectively. These observed peaks could be assigned to $Ni^{2+}/Ni^{4+}$ electrochemical process.

The Nyquist plots of $LiNi_{1/2}Mn_{1/2}O_2$ at different SOC are shown in Fig.9. EIS experiments were performed on working electrodes at the open circuit voltage (OCV) state. Just one semicircle was observed in the OCV state for both samples. In the low frequency region a straight line was obtained which represents a diffusion-controlled process in the solid electrode. The semicircle might contain a contribution due to the compaction of particles in the composite cathode, i.e. the inter-particle contacts such as oxide-oxide, carbon-oxide and carbon-carbon contacts. Zsimpwin software was used to quantitatively analyze the condition of the electrode reaction, and the situation of electrode can be approxi-mately represented by the equivalent circuit in Fig.10. $R_l$ is the solution resistance of the cell, $R_{ct}$ is the cathode charge transfer resistance, $C_d$ represents the double layer capacitance, and $Z_w$ is diffusion impedance. Table 2 lists the results calculated from electrochemical impedance spectra based on the equivalent circuit shown in Fig.10 using Zsimpwin software.

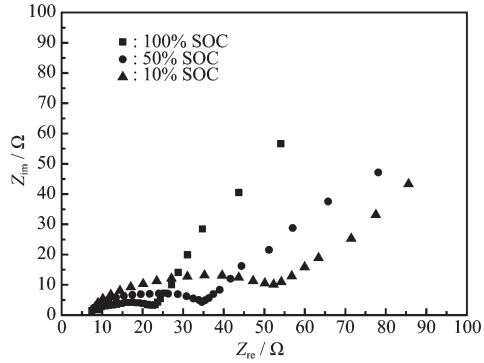


Fig.9　EIS spectra (Nyquist complex plane plots) for cells with active electrode of $LiNi_{1/2}Mn_{1/2}O_2$ at different SOC at the OCV state

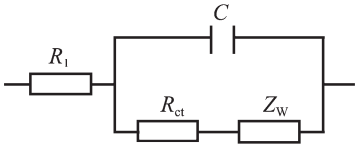


$R_l$ is the solution resistance of the cell, $R_{ct}$ is the cathode charge transfer resistance, $C_l$ represents the double layer capacitance, and $Z_w$ is a diffusion impedance

Fig.10　Equivalent circuit for $LiNi_{1/2}Mn_{1/2}O_2$ electrode

It is obvious that the material at lower SOC has a higher charge-transfer resistance ($R_{ct}$) and a higher $Z_w$, i.e. with the decreasing of SOC, $R_{ct}$ increases gradually.

**Table 2 Results of EIS analysis of the $LiMn_{1/2}Ni_{1/2}O_2$ at different states of charge**

| | $R_1$ / Ω | $C$ / F | $R_{ct}$ / Ω | $Z_w$ / ($\Omega^{-1}\cdot cm^{-2}\cdot s^{0.5}$) |
|---|---|---|---|---|
| 100% SOC | 8.34 | $2.257\times10^{-6}$ | 8.586 | 0.007 051 |
| 50% SOC | 9.255 | $1.217\times10^{-6}$ | 18.28 | 0.006 046 |
| 10% SOC | 10.03 | $1.082\times10^{-6}$ | 29.11 | 0.003 001 |

This may suggest that the lithium ions diffuse into the cathode more hardly. As the discharge process goes on (a process of SOC decreasing gradually), the amount of lithium increases in the cathode material and the surface lithium site of hexahedron is occupied by lithium ion. Continuous discharge, the lithium ions have to occupy the body site of $Li_{1-x}Ni_{1/2}Mn_{1/2}O_2$ that causes the coming lithium ion overcome the repelling force of electrostatics and overcome the block from the lithium occupied at lattice. Thus, the lithium ions to enter the lithium site of $LNi_{1/2}Mn_{1/2}O_2$ have to overcome larger lattice energy, i.e. $R_{ct}$ becomes bigger. But even at the end of discharge, the $R_{ct}$ is not very big. This indicates that the $LiNi_{1/2}Mn_{1/2}O_2$ has good ability of Li-ion diffusion.

## 3 Conclusion

We have demonstrated an improved route for synthesizing $LiNi_{1/2}Mn_{1/2}O_2$ under a simple condition. XRD analysis confirms a layered structure. The material synthesized at 900 ℃ for 9 h in air exhibits stable capacities of about 140 $mAh\cdot g^{-1}$ in the voltage range of 2.8~4.6 V at the end of 40 cycles, indicating a better electrochemical performance. The two oxidation peaks of the first time voltammetry curve show that the material has irreversible phase change because of the existing of $Ni^{3+}$ and $Mn^{3+}$. With the increasing of cycling numbers, the structure of $LiNi_{1/2}Mn_{1/2}O_2$ becomes stable. The smaller resistance of electrochemical impedance results shows that the material has good Li-ion diffusion ability.

## References:


[1] Nitta Y, Okamura K, Haraguchi K, et al. *J. Power Sources*, **1995**,**54**:511~515

[2] Yoshio M, Todorov Y, Yamato K, et al. *J. Power Sources*, **1998**,**74**(1):46~53

[3] Ohzuku T, Makimura Y. *Chem. Lett.*, **2001**,(8):744~745

[4] Reed J, Ceder G. *Solid-State Lett.*, **2002**,**5**(7):A145~A148

[5] Makimura Y, Nakayama N, Ohzuku T. *Proceedings-Electrochemical Soc.*, **2003**,(20):261~268

[6] Zhang L, Noguchi H, Yoshio M. *J. Power Sources*, **2002**,**110**: 57~64

[7] Kang S H, Kim J, Stoll M E, et al. *J. Power Sources*, **2002**,**112** (1):41~48

[8] Wu Q, Li X L, Yan M M, et al. *Electrochem. Communi.*, **2003**, **5**:878~882

[9] Makimura Y, Ohzuku T. *J. Power Sources*, **2003**,**119~121**:156 ~160

[10]Shaju K M, Subba Rao G V, Chowdari B V R. *Electrochi. Acta*, **2003**,**48**:1505~1514

[11]Gopukumar S, Chung K Y. *Electrochi. Acta*, **2004**,**49**:803~ 810

[12]Zhang X F, Wen Z Y, Zhu X J, et al. *Materials Letters*, **2006**, **60**(12):1470~1474

[13]Park S H, Kang S H, Johnson C S, et al. *Electrochem. Communi.*, **2007**,**9**(2):262~268

[14]Cushing B L, Goodenough J B. *Solid State Sciences*, **2002**,**4** (11~12):1487~1493

[15]Kang S H, Amine K. *J. Power Sources*, **2003**,**119~121**:150~ 155

[16]Johnson C S, Kim J S, Kropf A J, et al. *J. Power Sources*, **2003**,**119~121**:139~144

[17]Yoon W S, Paik Y, Yang X Q, et al. *J. Electrochem. Solid-State Lett.*, **2002**,**5**(11): A263~A266

[18]Lu Z, Beaulieu L Y, Donaberger R A, et al. *J. Electrochem. Soc.*, **2002**,**149**:A778~A791